

# Older than they look: Cryptic recycled xenotime on detrital zircon

Maximilian Dröllner<sup>1,\*</sup>, Milo Barham<sup>1</sup>, Christopher L. Kirkland<sup>1</sup>, and Malcolm P. Roberts<sup>2</sup>

<sup>1</sup>Timescales of Mineral Systems Group, The Institute of Geoscience Research, School of Earth and Planetary Sciences, Curtin University, GPO Box U1987, Perth, WA 6845, Australia

<sup>2</sup>Centre for Microscopy, Characterisation and Analysis, The University of Western Australia, Perth, WA 6009, Australia

## ABSTRACT

Dating of xenotime outgrowths (XOs) has been used to obtain depositional age constraints on sedimentary sequences devoid of volcanic tuffs and biostratigraphically useful fossils (i.e., most of Earth history). Here, we present geochronological and geochemical data from XOs on detrital zircon from the Early Cretaceous Broome Sandstone, NW Australia. Ages of XOs predate the palynologically constrained deposition of the Broome Sandstone by at least 150 m.y., suggesting that these XOs were detrital and transported together with the zircon to which they are attached. This finding contrasts with the general assumption that XOs are principally authigenic phases. Integration of geochronology and geochemistry links Broome Sandstone XOs to intermediate geological events in the sediment source area. These results emphasize the importance of evaluating a potential detrital origin for XOs because sedimentary transport does not appear to universally destroy nor liberate them from their zircon substrate. Despite this, the study of XOs provides an important means to reconstruct complexities of source-to-sink sediment histories, including intermediate storage and overprinting, e.g., during diagenetic, metamorphic, hydrothermal, and igneous activity. Such information is critical for more holistic geological reconstructions but is not retained within the most applied provenance tool (detrital zircon).

## INTRODUCTION

U-Pb dating of authigenic xenotime outgrowths (XOs) on detrital zircon (DZ) grains (Rasmussen, 1996) has been widely applied to temporally constrain geological processes and biological evolution through deep time (McNaughton et al., 1999; Lan, 2022). This geochronometer has proven to be especially important to help construct stratigraphic frameworks in the Precambrian (François et al., 2017; Zhang et al., 2022), an interval notoriously lacking reliable absolute dating methods for diagenetic processes and sedimentary packages more generally. As such, XO geochronology has been employed to determine the time of deposition of sediments, which is critical to resolve a variety of questions in earth science, particularly

involving the evolutionary time line of eukaryotes (Rasmussen et al., 2004; Lan et al., 2014).

It is generally accepted that XOs in unmetamorphosed and low-grade metamorphic sedimentary rocks represent an authigenic phase (i.e., formed during syn- or postdepositional processes in the sediment in which they occur); this contrasts with detrital xenotime grains, which are typically of igneous origin (Kositcin et al., 2003). A common argument to support authigenic growth is the apparent fragility of small (<20 μm), characteristically pyramidal outgrowths (Hetherington et al., 2008; Hay and Dempster, 2009) and observations of dislodged XOs during sample handling (Rasmussen, 2005). Thus, preservation of XOs during sediment recycling would have implications for their current application as authigenic age constraints on the lithostratigraphic unit in which they occur. Conversely, recognizing the retention of XOs through sedimentary transportation could offer information on intermediate grain histories, like that recently demonstrated by monazite (Moecher et al., 2019; Aleinikoff


et al., 2023). Ultimately, tracking these intermediate processes, typically not captured in the DZ record, is important for the reconstruction of ancient sediment pathways.


This study presents U-Pb geochronology and geochemistry of XOs, apparent xenotime inclusions (and associated DZ substrate and host, respectively), and detrital xenotime grains found in Early Cretaceous littoral and poorly consolidated sediments in NW Australia. We reconsider a combined detrital origin of the XOs and their DZ substrates, discuss the implications for relying on XO age data to constrain depositional processes, and illustrate the application of XOs to reconstruct polyphase grain histories.

## MATERIALS AND METHODS

This study focused on samples from the Early Cretaceous Broome Sandstone (ca. 140–127 Ma; Smith et al., 2013) of the Canning Basin, NW Australia (Fig. 1). The Broome Sandstone consists of a range of sand and sandstone lithologies dominated by well-sorted and rounded, fine to very fine quartz-rich detritus deposited in a shallow-marine to paralic environment (Boyd and Teakle, 2016; Salisbury et al., 2016). Three samples originated from the Thunderbird heavy mineral deposit (Table S1 of the Supplemental Material<sup>1</sup>), where siliciclastic sediments are poorly consolidated and friable, removing the need for potentially destructive sample crushing or similar processing techniques. The other Broome Sandstone sample was collected from an outcropping indurated sandstone (Table S1) and subjected to high-voltage electrical fragmentation. Zircon grains were concentrated using a water-shaking table, heavy liquid separation, and magnetic separation. Mineral separates were embedded into epoxy resin, ground to expose grain interiors, and polished.

Automated mineral identification using a scanning electron microscope equipped with

Maximilian Dröllner  <https://orcid.org/0000-0001-8661-9565>

Milo Barham  <https://orcid.org/0000-0003-0392-7306>

Christopher L. Kirkland  <https://orcid.org/0000-0003-3367-8961>  
\*maximilian.droellner@curtin.edu.au

<sup>1</sup>Supplemental Material. Supplemental Material S1 (detailed analytical methods) and Supplemental Material S2 (data in Tables S1–S7). Please visit <https://doi.org/10.1130/G51178.1> to access the supplemental material, and contact editing@geosociety.org with any questions.



**Figure 1. Overview of sample locations and crustal units discussed in this work. Area between red dashed lines was affected by Alice Springs Orogeny (after Klootwijk, 2013). AB—Amadeus Basin; AR—Arunta region; MP—Musgrave Province.**

energy-dispersive X-ray spectrometers mapped the occurrences of xenotime and zircon in mounted samples. Laser ablation–inductively coupled plasma–mass spectrometry (LA-ICP-MS) and secondary ion mass spectrometry (SIMS) measurements of the U–Pb isotopic composition of xenotime and DZ were conducted at Curtin University’s John de Laeter Centre, Perth, Western Australia. All ages are concordia ages, and uncertainties are at the  $2\sigma$  level. Dating was followed by geochemical characterization using an electron probe microanalyzer (EPMA) at the Centre for Microscopy, Characterisation and Analysis at The University of Western Australia, Perth. XOs required small analytical spots ( $\sim 7\ \mu\text{m}$  for LA-ICP-MS with pit depths of  $\sim 3\ \mu\text{m}$ ;  $\sim 8 \times 7\ \mu\text{m}$  for SIMS with pit depths of  $\sim 1\ \mu\text{m}$ ) and individual assess-

ment of the potential of xenotime-zircon analytical mixtures. This quality control included examination of the analytical pits (Fig. 2) and monitoring of Zr content. Mixed xenotime-zircon analyses commonly showed increased levels of Zr compared to pure xenotime analyses, which showed low Zr contents consistent with EPMA measurements (Table S7). Measurements showing evidence for analytical mixtures were excluded from later interpretations. Details of the sample preparation, mineral identification, and geochronological and geochemical methods are provided in Supplemental Material S1 (see footnote 1).

## RESULTS

Automated mineral identification revealed rare XOs on DZ substrate ( $<1\%$  of  $>150,000$  scanned DZ grains; Figs. 2A and 2B; Fig. S1), apparent xenotime inclusions within DZ (Fig. 2C; Fig. S1), and detrital xenotime grains (up to  $100\ \mu\text{m}$ ; Fig. S1). Broome Sandstone XOs showed subhedral to anhedral shapes, were up to  $20\ \mu\text{m}$  in size, and occurred on subrounded DZ (Figs. 2A and 2B). The six youngest analyses of XOs without evidence of analytical mixtures with zircon defined a distinct age group (Figs. 3A and 3B). U–Pb ages of these uncontaminated xenotime analyses, interpreted as growth ages based on the high radiogenic Pb retentivity (Cherniak, 2010), ranged from  $446 \pm 39\ \text{Ma}$  to  $297 \pm 10\ \text{Ma}$  and were younger than those from mixed xenotime-zircon analyses (Fig. 3B; Fig. S1). The ages of XOs and their respective DZ substrates differed significantly; e.g., xenotime X4 (coding is from Tables S2–S7 in Supplemental Material S2, where X = xenotime and Z = zircon) yielded an age of  $410 \pm 19\ \text{Ma}$  (mean square of weighted deviates [MSWD] = 1.3,  $n = 2$ ), whereas the DZ substrate Z4 yielded an age of  $968 \pm 19\ \text{Ma}$ . In contrast, ages of interpreted xenotime inclusions (Fig. 2C), possibly exposed due to grain fracturing or abrasion during sedimentary trans-

port or sample preparation, were indistinguishable from their zircon host; e.g., X8 had an age of  $1186 \pm 32\ \text{Ma}$  compared to the age of  $1191 \pm 13\ \text{Ma}$  for Z8. Both XO-bearing DZ and detrital xenotime grains revealed polymodal age spectra dominated by Proterozoic ages (Fig. S2).

Generally, chondrite-normalized rare earth element (REE) contents in xenotime from this study increased toward heavier REEs (except Eu) but flattened from Dy onward (Fig. 3C; Table S7). Outgrowths X4, X5, and X6 showed a pronounced negative Eu anomaly, whereas X1 and X2 did not have strong Eu anomalies (X7 Eu was below the detection limit). The apparent xenotime inclusion X8 yielded the most pronounced negative Eu anomaly among analyses of composite grains. All but two detrital xenotime grains showed significant negative Eu anomalies, consistent with detrital xenotime having lower Eu values than XOs (Fig. 3D). Overall, the shape of REE patterns of detrital xenotime resembled that of most XOs (Fig. 3E).

## DISCUSSION

### Detrital Origin of Xenotime Outgrowths

The formation of XOs at ca. 446–297 Ma (Figs. 3A and 3B) clearly predated the ca. 140–127 Ma depositional age of the Broome Sandstone defined by palynology (i.e., dinofossils, pollen, and spores; Smith et al., 2013) and plant macrofossils (McLoughlin, 1996). This observation conclusively demonstrates that all the identified XOs on DZ did not form within the Broome Sandstone as authigenic phases. The timing of XO formation is not compatible with known proximal geological events, instead implying more significant sedimentary transport and redeposition after their growth, consistent with previous interpretations of Canning Basin sediment originating from central Australia (Haines et al., 2013; Morón et al., 2019; Dröllner et al., 2023). Thus, the XO age signature is best explained by a detrital origin, similar to their associ-

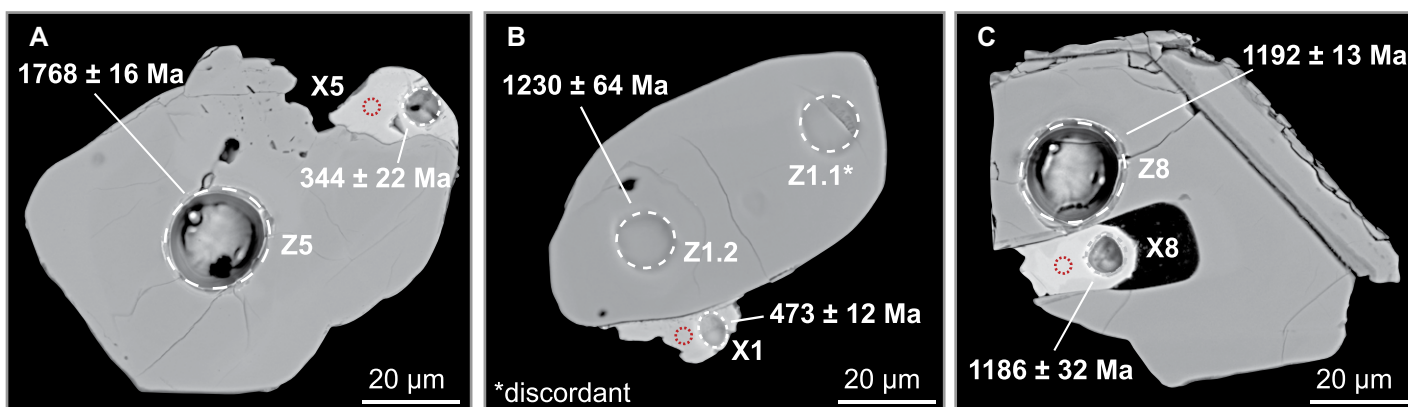


**Figure 2. Backscattered electron images of zircon (Z) and xenotime (X) analyzed using (A) laser ablation–inductively coupled plasma–mass spectrometry (LA-ICP-MS) and (B) secondary ion mass spectrometry (SIMS). (C) Apparent xenotime inclusion (and detrital zircon [DZ] host). White and red circles indicate analytical spots for U–Pb and electron probe microanalyzer (EPMA) analysis, respectively.**

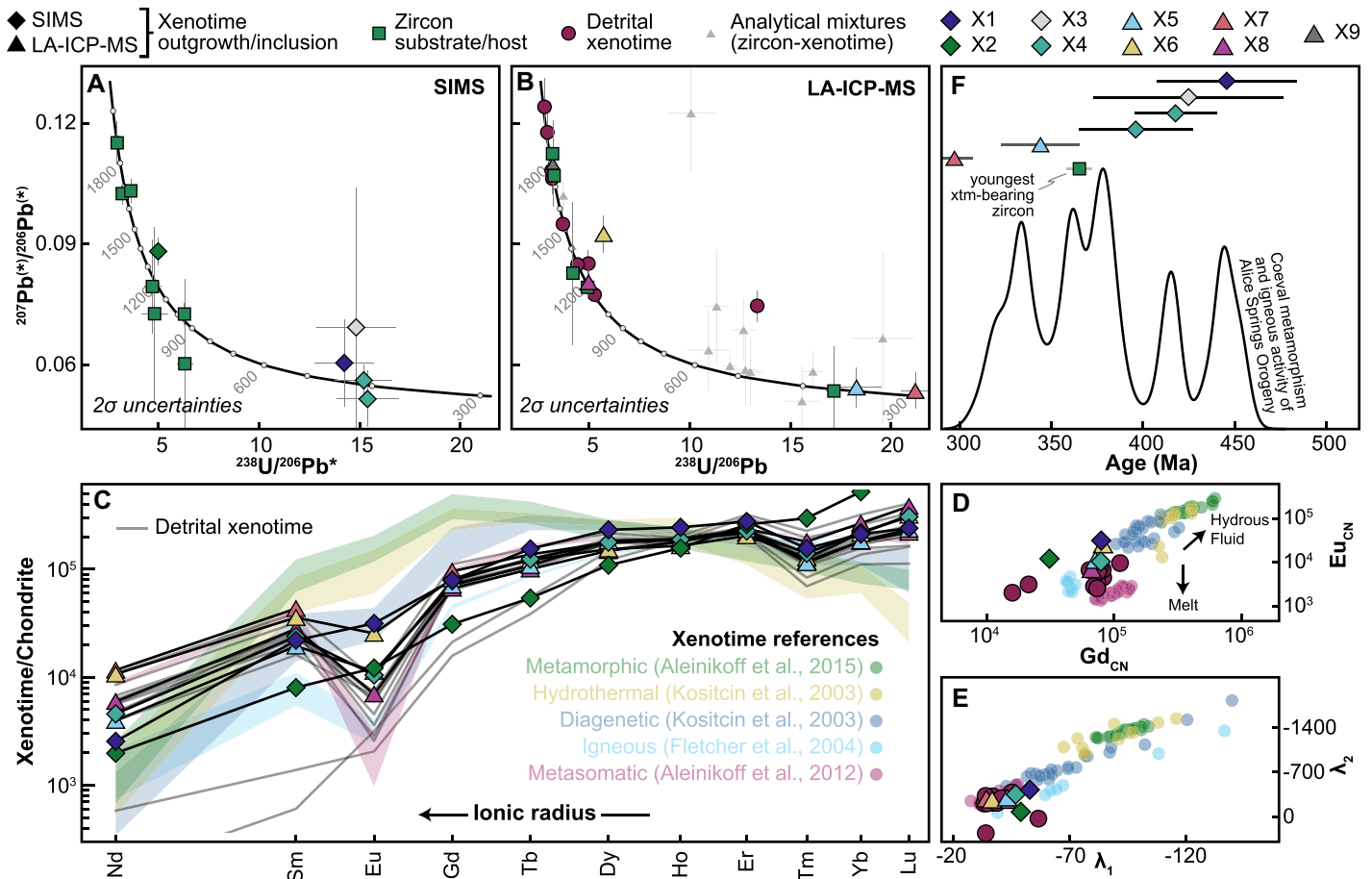


**Figure 3.** (A) Secondary ion mass spectrometry (SIMS) and (B) laser ablation–inductively coupled plasma–mass spectrometry (LA-ICP-MS) concordia diagrams of xenotime and zircon geochronology. Asterisks (\*) indicate only SIMS data (A) corrected for common Pb. (C) Chondrite-normalized (CN) rare earth element (REE) patterns of xenotime analyses. Transparent envelopes show characteristic REE patterns (mean; 1 standard deviation [SD]) from xenotime references from different environments. (D)  $Eu_{CN}$  vs.  $Gd_{CN}$  scatterplot of xenotime outgrowths (XOs) and reference data and interpretation after Kositsin et al. (2003). (E) REE shape coefficients (O’Neill, 2016)  $\lambda_1$  (slope) and  $\lambda_2$  (quadratic curvature), ignoring anomalous Eu, compared to reference data. (F) Comparison of xenotime (xtm) outgrowth ages and pooled zircon density estimate of mineral (zircon, monazite, titanite, garnet, phyllosilicates) and whole-rock ages of Alice Springs Orogeny (equal weights for each group; compilation of Piazzolo et al., 2020).

ated zircon substrate. XO survival during sedimentary transport is consistent with their subhedral to anhedral shapes but incompatible with their commonly assumed fragility (e.g., Rasmussen, 2005; Hay and Dempster, 2009). A possible geological control explaining the preservation of XOs is shielding of xenotime-bearing grains within rock fragments or grain coatings during transportation. However, there were no rock fragments in the analyzed samples, nor were grain coatings detected, providing no evidence for shielding as a preservation mechanism. A perhaps more important facet governing preservation of XOs in the Broome Sandstone is the unconsolidated nature of the sample material, which precluded the need for destructive processing techniques (e.g., crushing). Moreover, the high concentration of zircon (~1% of the bulk sample; Boyd and Teakle, 2016), in tandem with automated phase identification (>10,000 DZ grains per mount scanned for 14 mounts), facilitated a greater opportunity for identification of

unusual preservation styles of detrital XOs (compared to conventional manual selection; Lan, 2022). Significantly, the XO grains studied herein survived enhanced physical attrition in a littoral depositional system associated with the upgrading processes necessary to form economic concentrations of placer heavy mineral sands (Boyd and Teakle, 2016).

The age discrepancy identified in this work between xenotime formation and the age of deposition is consistent with previous indications of recycled XOs (Zhang et al., 2022) and demonstrates a possibly significant pitfall in the interpretation of presumed authigenic xenotime. Although other indicators (e.g., palynology) in relatively young rocks (this study) can assist with age interpretations, similar information is usually absent for older, particularly Precambrian, rocks often targeted for xenotime geochronology (Matteini et al., 2012). Therefore, detailed evaluation of chemistry (Lan et al., 2013), (micro-)textures (Vallini et al., 2005), and/or relationships to authigenic phases (Drost

et al., 2013) is critical to establish a truly authigenic origin and/or reasonably preclude a detrital origin for XOs.

### Intermediate Processes and Transient Sediment Storage Revealed by Xenotime Outgrowths

The dominant sources for Broome Sandstone accessory minerals are in central Australia, namely, the Musgrave Province, the Arunta region, and the Amadeus Basin (Fig. 1; Fig. S2; Dröllner et al., 2023). Similarly, the youngest group of XOs in the Broome Sandstone is interpreted to have been derived from central Australia, since their ages match the timing of the 450–300 Ma Alice Springs Orogeny (Buick et al., 2008). This interpretation is consistent with the similarity of the age spectrum of the xenotime-bearing DZ and that of the bulk DZ of the Broome Sandstone (Fig. S2; Dröllner et al., 2023) based on a Kolmogorov-Smirnov test ( $D = 0.2$ ), implying that detrital XOs can reveal source-to-sink relationships.

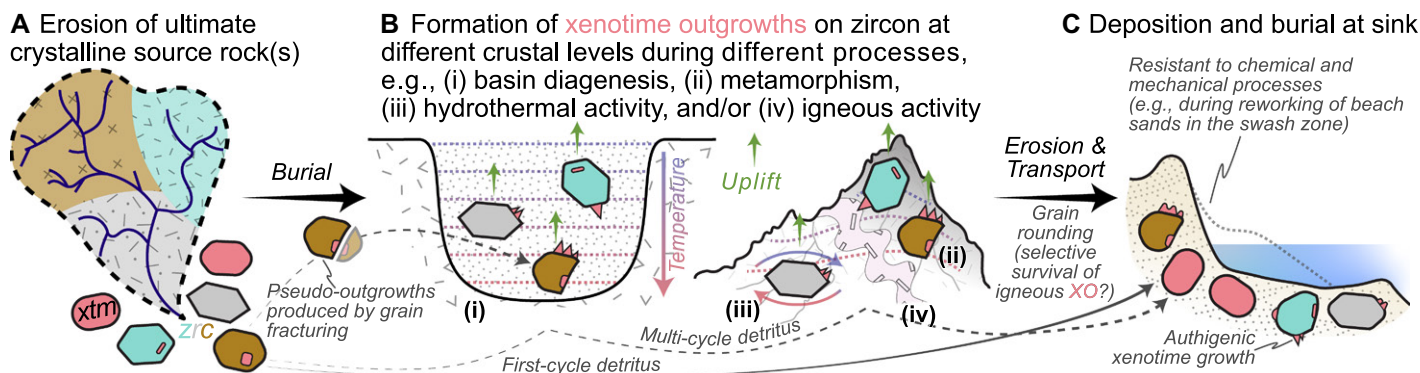


**Figure 4. Schematic illustration of processes described herein. This includes (A) initial erosion of crystalline sources that liberates zircon (zrc), which may be routed directly to its sink (first cycle) or alternatively follow multicycle pathways, possibly evidencing (B) formation of xenotime (xtm) outgrowths in intermediate sources during different processes, preceding (C) deposition at sink.**

Since the geochemical fingerprint of xenotime (Fig. 3C) is a function of its growth environment (Lan et al., 2013), detrital xenotime geochemistry can help to define intermediate processes in the sediment source area. The Alice Springs Orogen records multiple episodes of pegmatite emplacement and coeval tectonic deformation (Piazolo et al., 2020), as well as metasomatic (Raimondo et al., 2011) and hydrothermal activity (Schoneveld et al., 2015). Xenotime grown from hydrous fluids is distinct to xenotime formed in igneous settings and shows increasing Eu with increasing Gd concentrations (Fig. 3D; Kositcin et al., 2003). This geochemical trend of hydrothermal or diagenetic fluid growth was not apparent in XOs of this study, which showed lower Eu concentrations characteristic of melt derivation. A potential melt origin is also consistent with the REE shape coefficients (Fig. 3E), where XOs and detrital xenotime resembled both igneous xenotime and metasomatic xenotime. However, XOs from the Broome Sandstone had lower U and Th concentrations than metasomatism-derived xenotime (~0.4 and 0.3 vs. 2.2 and 0.6 wt%, respectively; Aleinikoff et al., 2012), which have never previously been observed as outgrowths. Conversely, xenotime-zircon intergrowths occur in (meta-) igneous rocks (Budzyń et al., 2018) and make an igneous origin for XOs the favored interpretation, based on the limited compositional data set. Overall, the XO geochemical data herein contrast with data of xenotime derived from hydrous fluids or metamorphism (Figs. 3D and 3E), and Broome Sandstone XO genesis is best explained by formation in association with Alice Springs Orogeny magmas.

These findings suggest that xenotime geochronology can refine polyphase grain histories in sedimentary units (Fig. 4). Erosion of crystalline basement (Fig. 4A) may result in directly captured first-cycle detritus (e.g., detrital xenotime grains), while a significant part of the resilient DZ may experience multiple episodes of intermediate storage, burial, and uplift (multicycle detritus). Multicycle DZ may experience

a range of conditions at different crustal levels, perhaps acting as a nucleus for XOs (Fig. 4B), e.g., during diagenetic, metamorphic, hydrothermal, and igneous processes. Notably, the igneous-detrital origin of all the XOs in this study may suggest differential mechanical resistance of XOs according to their growth environment, implying selective survival of XOs formed during igneous processes. Ultimately, XOs can provide direct evidence of complex intermediate processes influencing detritus. Recognizing such multicyclicity is important because sediment recycling can induce bias in the interpretation of DZ data (Moecher et al., 2019). Furthermore, XOs reveal detritus from sources with scarce igneous activity that are typically underrepresented based on other proxies (e.g., DZ; Fig. S2), but which are critical for source-to-sink reconstructions. Overall, these results suggest that XOs represent a possible novel complementary tool to characterize intermediate storage episodes and sediment recycling.

## CONCLUSIONS

High-throughput automated mineral identification detected XOs on DZ from the Broome Sandstone, suggesting that XOs can be resistant to sedimentary processes. Therefore, the geochemistry and age constraints on XOs need to be carefully evaluated to determine the possibility of a detrital origin as a viable alternative to authigenic growth within the host sediment. Where a detrital origin for XOs can be confirmed, XOs may represent a useful means to understand complex grain histories and, hence, more holistic reconstructions of ancient sedimentary systems.

## ACKNOWLEDGMENTS

This research was supported by Minerals Research Institute of Western Australia (MRIWA) grant M551 and The Institute for Geoscience Research (Curtin University). Part of this research was undertaken using electron microscope instrumentation (ARC LE140100150) at the John de Laeter Centre (JdLC), Curtin University. Research in the GeoHistory Facility, JdLC is enabled by AuScope (auscope.org.au) and the Australian Government via the National Collaborative

Research Infrastructure Strategy (NCRIS). The authors acknowledge the facilities, and the scientific and technical assistance of Microscopy Australia at the Centre for Microscopy, Characterisation & Analysis, The University of Western Australia, a facility funded by the University, State and Commonwealth Governments. We thank the Yawuru community and the Shire of Broome for access to land, Rohan Hine and David Sleight of Iluka Resources for discussions, Seb Gray and Sheffield Resources for samples, Urs Schaltegger for editorial handling, and Zhongwu Lan, John N. Aleinikoff, Kevin Mahan, and an anonymous reviewer for constructive journal reviews.

## REFERENCES CITED

- Aleinikoff, J.N., Grauch, R.I., Mazdab, F.K., Kwak, L., Fanning, C.M., and Kamo, S.L., 2012, Origin of an unusual monazite-xenotime gneiss, Hudson Highlands, New York: SHRIMP U-Pb geochronology and trace element geochemistry: *American Journal of Science*, v. 312, no. 7, p. 723–765, <https://doi.org/10.2475/07.2012.02>.
- Aleinikoff, J.N., Lund, K., and Fanning, C.M., 2015, SHRIMP U-Pb and REE data pertaining to the origins of xenotime in Belt Supergroup rocks: Evidence for ages of deposition, hydrothermal alteration, and metamorphism: *Canadian Journal of Earth Sciences*, v. 52, no. 9, p. 722–745, <https://doi.org/10.1139/cjes-2014-0239>.
- Aleinikoff, J.N., Southworth, C.S., and Fanning, C.M., 2023, SHRIMP U-Pb geochronology of Mesoproterozoic basement and overlying Ocoee Supergroup, NC-TN: Dating diagenetic xenotime and monazite overgrowths on detrital minerals: *Canadian Journal of Earth Sciences* (in press), <https://doi.org/10.1139/cjes-2022-0093>.
- Boyd, D.M., and Teakle, M.G., 2016, Thunderbird heavy mineral sand deposit, Western Australia: *Transactions of the Institution of Mining and Metallurgy Section B—Applied Earth Science*, v. 125, no. 3, p. 128–139, <https://doi.org/10.1080/03717453.2016.1200268>.
- Budzyń, B., Sláma, J., Kozub-Budzyń, G.A., Konečný, P., Holický, I., Rzepa, G., and Jastrzębski, M., 2018, Constraints on the timing of multiple thermal events and re-equilibration recorded by high-U zircon and xenotime: Case study of pegmatite from Piława Górna (Góry Sowie block, SW Poland): *Lithos*, v. 310–311, p. 65–85, <https://doi.org/10.1016/j.lithos.2018.03.021>.
- Buick, I.S., Storkey, A., and Williams, I.S., 2008, Timing relationships between pegmatite emplacement, metamorphism and deformation during the intra-plate Alice Springs Orogeny, central Australia: *Journal of Metamorphic Geology*,

- v. 26, no. 9, p. 915–936, <https://doi.org/10.1111/j.1525-1314.2008.00794.x>.
- Cherniak, D.J., 2010, Diffusion in accessory minerals: Zircon, titanite, apatite, monazite and xenotime: *Reviews in Mineralogy and Geochemistry*, v. 72, no. 1, p. 827–869, <https://doi.org/10.2138/rmg.2010.72.18>.
- Dröllner, M., Barham, M., and Kirkland, C.L., 2023, Reorganization of continent-scale sediment routing based on detrital zircon and rutile multi-proxy analysis: *Basin Research*, v. 35, no. 1, p. 363–386, <https://doi.org/10.1111/bre.12715>.
- Drost, K., Wirth, R., Košler, J., Fonneland Jørgensen, H., and Ntaflou, T., 2013, Chemical and structural relations of epitaxial xenotime and zircon substratum in sedimentary and hydrothermal environments: A TEM study: *Contributions to Mineralogy and Petrology*, v. 165, no. 4, p. 737–756, <https://doi.org/10.1007/s00410-012-0833-6>.
- Fletcher, I.R., McNaughton, N.J., Aleinikoff, J.A., Rasmussen, B., and Kamo, S.L., 2004, Improved calibration procedures and new standards for U-Pb and Th-Pb dating of Phanerozoic xenotime by ion microprobe: *Chemical Geology*, v. 209, no. 3–4, p. 295–314, <https://doi.org/10.1016/j.chemgeo.2004.06.015>.
- François, C., Baludikay, B.K., Storme, J.Y., Baudet, D., Paquette, J.L., Fialin, M., and Javaux, E.J., 2017, Contributions of U-Th-Pb dating on the diagenesis and sediment sources of the lower group (BI) of the Mbuji-Mayi Supergroup (Democratic Republic of Congo): *Precambrian Research*, v. 298, p. 202–219, <https://doi.org/10.1016/j.precamres.2017.06.012>.
- Haines, P.W., Wingate, M.T.D., and Kirkland, C.L., 2013, Detrital zircon U-Pb ages from the Paleozoic of the Canning and Officer Basins, Western Australia: Implications for provenance and inter-basin connections, *in* Keep, M., and Moss, S.J., eds., *The Sedimentary Basins of Western Australia IV: Proceedings of the Petroleum Exploration Society of Australia Symposium*, Perth, Western Australia: Perth, Petroleum Exploration Society of Australia.
- Hay, D.C., and Dempster, T.J., 2009, Zircon alteration, formation and preservation in sandstones: *Sedimentology*, v. 56, no. 7, p. 2175–2191, <https://doi.org/10.1111/j.1365-3091.2009.01075.x>.
- Hetherington, C.J., Jercinovic, M.J., Williams, M.L., and Mahan, K., 2008, Understanding geologic processes with xenotime: Composition, chronology, and a protocol for electron probe microanalysis: *Chemical Geology*, v. 254, no. 3–4, p. 133–147, <https://doi.org/10.1016/j.chemgeo.2008.05.020>.
- Klootwijk, C., 2013, Middle–late Paleozoic Australia-Asia convergence and tectonic extrusion of Australia: *Gondwana Research*, v. 24, no. 1, p. 5–54, <https://doi.org/10.1016/j.gr.2012.10.007>.
- Kositcin, N., McNaughton, N.J., Griffin, B.J., Fletcher, I.R., Groves, D.I., and Rasmussen, B., 2003, Textural and geochemical discrimination between xenotime of different origin in the Archaean Witwatersrand Basin, South Africa: *Geochimica et Cosmochimica Acta*, v. 67, no. 4, p. 709–731, [https://doi.org/10.1016/S0016-7037\(02\)01169-9](https://doi.org/10.1016/S0016-7037(02)01169-9).
- Lan, Z., 2022, Authigenic monazite and xenotime Pb-Pb/U-Pb dating of siliciclastic sedimentary rocks: *Earth-Science Reviews*, v. 234, <https://doi.org/10.1016/j.earscirev.2022.104217>.
- Lan, Z., Li, X., Chen, Z.-Q., Li, Q., Hofmann, A., Zhang, Y., Zhong, Y., Liu, Y., Tang, G., Ling, X., and Li, J., 2014, Diagenetic xenotime age constraints on the Sanjiaotang Formation, Luoyu Group, southern margin of the North China craton: Implications for regional stratigraphic correlation and early evolution of eukaryotes: *Precambrian Research*, v. 251, p. 21–32, <https://doi.org/10.1016/j.precamres.2014.06.012>.
- Lan, Z.-W., Chen, Z.-Q., Li, X.-H., Li, B., and Adams, D., 2013, Hydrothermal origin of the Paleoproterozoic xenotime from the King Leopold Sandstone of the Kimberley Group, Kimberley, NW Australia: Implications for a ca 1.7 Ga far-field hydrothermal event: *Australian Journal of Earth Sciences*, v. 60, no. 4, p. 497–508, <https://doi.org/10.1080/08120099.2013.806360>.
- Matteini, M., Dantas, E.L., Pimentel, M.M., de Alvarenga, C., and Dardenne, M.A., 2012, U-Pb and Hf isotope study on detrital zircons from the Paranoá Group, Brasília belt, Brazil: Constraints on depositional age at Mesoproterozoic-Neoproterozoic transition and tectono-magmatic events in the São Francisco craton: *Precambrian Research*, v. 206–207, p. 168–181, <https://doi.org/10.1016/j.precamres.2012.03.007>.
- McLoughlin, S., 1996, Early Cretaceous macrofloras of Western Australia: Records of the Western Australian Museum, v. 18, p. 19–65.
- McNaughton, N.J., Rasmussen, B., and Fletcher, I.R., 1999, SHRIMP uranium-lead dating of diagenetic xenotime in siliciclastic sedimentary rocks: *Science*, v. 285, no. 5424, p. 78–80, <https://doi.org/10.1126/science.285.5424.78>.
- Moecher, D.P., Kelly, E.A., Hietspas, J., and Samson, S.D., 2019, Proof of recycling in clastic sedimentary systems from textural analysis and geochronology of detrital monazite: Implications for detrital mineral provenance analysis: *Geological Society of America Bulletin*, v. 131, no. 7–8, p. 1115–1132, <https://doi.org/10.1130/B31947.1>.
- Morón, S., Cawood, P.A., Haines, P.W., Gallagher, S.J., Zahirovic, S., Lewis, C.J., and Moresi, L., 2019, Long-lived transcontinental sediment transport pathways of East Gondwana: *Geology*, v. 47, no. 6, p. 513–516, <https://doi.org/10.1130/G45915.1>.
- O’Neill, H.S.C., 2016, The smoothness and shapes of chondrite-normalized rare earth element patterns in basalts: *Journal of Petrology*, v. 57, no. 8, p. 1463–1508, <https://doi.org/10.1093/petrology/egw047>.
- Piazolo, S., Daczko, N.R., Silva, D., and Raimondo, T., 2020, Melt-present shear zones enable intracontinental orogenesis: *Geology*, v. 48, no. 7, p. 643–648, <https://doi.org/10.1130/G47126.1>.
- Raimondo, T., Clark, C., Hand, M., and Faure, K., 2011, Assessing the geochemical and tectonic impacts of fluid-rock interaction in mid-crustal shear zones: A case study from the intracontinental Alice Springs orogen, central Australia: *Journal of Metamorphic Geology*, v. 29, no. 8, p. 821–850, <https://doi.org/10.1111/j.1525-1314.2011.00944.x>.
- Rasmussen, B., 1996, Early-diagenetic REE-phosphate minerals (florencite, gorceixite, crandallite, and xenotime) in marine sandstones: A major sink for oceanic phosphorus: *American Journal of Science*, v. 296, no. 6, p. 601–632, <https://doi.org/10.2475/ajs.296.6.601>.
- Rasmussen, B., 2005, Radiometric dating of sedimentary rocks: The application of diagenetic xenotime geochronology: *Earth-Science Reviews*, v. 68, no. 3–4, p. 197–243, <https://doi.org/10.1016/j.earscirev.2004.05.004>.
- Rasmussen, B., Fletcher, I.R., Bengtson, S., and McNaughton, N.J., 2004, SHRIMP U-Pb dating of diagenetic xenotime in the Stirling Range Formation, Western Australia: 1.8 billion year minimum age for the Stirling biota: *Precambrian Research*, v. 133, no. 3–4, p. 329–337, <https://doi.org/10.1016/j.precamres.2004.05.008>.
- Salisbury, S.W., Romilio, A., Herne, M.C., Tucker, R.T., and Nair, J.P., 2016, The dinosaurian ichnofauna of the Lower Cretaceous (Valanginian–Barremian) Broome Sandstone of the Walmadany area (James Price Point), Dampier Peninsula, Western Australia: *Journal of Vertebrate Paleontology*, v. 36, supplement 1, p. 1–152, <https://doi.org/10.1080/02724634.2016.1269539>.
- Schoneveld, L., Spandler, C., and Hussey, K., 2015, Genesis of the central zone of the Nolans Bore rare earth element deposit, Northern Territory, Australia: *Contributions to Mineralogy and Petrology*, v. 170, no. 2, <https://doi.org/10.1007/s00410-015-1168-x>.
- Smith, T.E., Edwards, D.S., Kelman, A.P., Laurie, J.R., Le Poidevin, S., Nicoll, R.S., Mory, A.J., Haines, P.W., and Hocking, R.M., 2013, Canning Basin Biozonation and Stratigraphy: *Geoscience Australia Chart 31*, 1 p., [https://www.researchgate.net/publication/303824187\\_Canning\\_Basin\\_Biozonation\\_and\\_Stratigraphy](https://www.researchgate.net/publication/303824187_Canning_Basin_Biozonation_and_Stratigraphy) (accessed 1 May 2023).
- Vallini, D.A., Rasmussen, B., Krapez, B., Fletcher, I.R., and McNaughton, N.J., 2005, Microtextures, geochemistry and geochronology of authigenic xenotime: Constraining the cementation history of a Palaeoproterozoic metasedimentary sequence: *Sedimentology*, v. 52, no. 1, p. 101–122, <https://doi.org/10.1111/j.1365-3091.2004.00688.x>.
- Zhang, S., Cao, R., Lan, Z., Li, Z., Zhao, Z., Wan, B., Guan, C., and Yuan, X., 2022, SIMS Pb-Pb dating of phosphates in the Proterozoic strata of SE North China craton: Constraints on eukaryote evolution: *Precambrian Research*, v. 371, <https://doi.org/10.1016/j.precamres.2022.106562>.

Printed in USA